Pergamon

Structural Engineering Review, Vol. 5, No. 4, pp. 301–307, 1993

0952–5807/93 $7.00 + 0.00

0952–5807(93)E0010–J

PREDICTION OF BRIDGE FLUTTER THROUGH USE OF FINITE ELEMENTS

UWE STAROSSEK
J. Muller International, 9444 Balboa Ave. #200, San Diego, CA 92123, U.S.A.

(*Received* 21 *October* 1992; *and accepted in revised form* 28 *August* 1993)

Abstract—Wind-induced flutter of bridges with streamlined, plate-like cross-sections occurs as coupled torsional and vertical oscillation. Prediction can possibly be facilitated by representing the spatial system by a generalized 2-DOF system. This may, however, be inadmissible or may lead to extremely conservative results if the modes of torsional and vertical vibration differ strongly. Flutter prediction should then be based on spatial modeling. Classical methods of aircraft engineering for solving the spatial problem proceed from differential equations of motion or make use of variational principles. For applications in bridge engineering, the finite-element concept proves to be more efficient. In this paper, two beam elements of different complexity are presented. Formulation and solution of the resulting MDOF equations of motion are described. Results of numerical calculations are stated.

NOTATION

$\mathbf{A}$	global aerodynamic matrix
$\mathbf{a}$	aerodynamic matrix of beam element
b	half chord of aerodynamic contour of bridge cross-section
$\mathbf{C}$	global damping matrix
$c_{hh}, c_{h\alpha}, c_{\alpha h}, c_{\alpha\alpha}$	complex aerodynamic-derivative functions
$\mathbf{F}$	global force vector
$\mathbf{f}$	nodal force vector of beam element
g	overall damping coefficient
h	vertical displacement
I	mass moment of inertia per unit length
i	imaginary unit
$\mathbf{K}$	global stiffness matrix
k	reduced frequency
l	length of beam element
$\mathbf{M}$	global mass matrix
m	mass per unit length
$\mathbb{R}$	set of real numbers
r	reduced mass radius of gyration
t	time
v	(critical) wind speed
x	coordinate along element axis
α	torsional displacement
$\boldsymbol{\Delta}$	global displacement vector
$\boldsymbol{\delta}$	nodal displacement vector of beam element
ε_{ij}	ratio of i-th torsional natural frequency to j-th vertical-bending natural frequency in vacuum
ζ	dimensionless critical wind speed
μ	relative density
ρ	density of fluid (air)
ψ_i	interpolation function for element displacements
ω	circular frequency (of flutter)
ω_{hi}	i-th vertical-bending natural circular frequency in vacuum
$\omega_{\alpha i}$	i-th torsional natural circular frequency in vacuum
$\tilde{\omega}$	dimensionless flutter frequency
$'$, $''$	designation of real or imaginary part of a complex quantity
$'$	differentiation with respect to x
$\dot{}$	differentiation with respect to time

Subscripts

D	due to structural damping
I	due to mass inertia
L	due to self-induced aerodynamic forces
S	due to stiffness

INTRODUCTION

Wind-induced flutter of bridges with plate-like, i.e. streamlined, cross-sections occurs as coupled torsional and vertical oscillation. (For a more complete definition of "plate-like" see Refs [1,2].) Prediction by means of a generalized 2-degree-of-freedom (2-DOF) system—if admissible—requires simultaneous solution of the two equations of motion for torsional and vertical displacement (a two-dimensional complex eigenvalue problem). Utilization of a generalized 2-DOF system may be inadmissible or may lead to extremely conservative results if the modes of torsional and vertical vibration in vacuum differ strongly,[3] or when other system or environmental peculiarities exist. (Examples of such situations are given at the end of this paper.) Flutter prediction should then be based on spatial modeling, which leads to a higher-order eigenvalue problem.

Classical methods of aircraft engineering for solving the spatial problem proceed from partial differential equations of motion or make use of variational principles.[4,5] Solution of the resulting eigenvalue problem usually involves the choice of a set of global displacement patterns and numerical evaluation of integrals which extend over the total structure. Such methods have also been employed in the aeroelastic investigation of suspension bridges.[6,7] Other methods based on differential equations are the transfer-matrix procedure[3] and the dynamic direct-stiffness method.[1]

In bridge engineering, progressively more intricate systems, such as cable-stayed girders, are used. On the other hand, structural parameters are nearly uniform along the bridge span. The finite-element (FE) concept seems to be more suitable for handling the analysis of such structures. In this paper, two beam elements of different complexity are presented which can be utilized for a linear flutter analysis of line-like structures. Formulation and solution of the resulting multi-degree-of-freedom (MDOF) equations of motion are described, and the results of numerical checks and investigations are stated.

FLUTTER CALCULATION BY MEANS OF FINITE ELEMENTS

Two finite beam elements

For modeling of a fluttering beam, the precision relative to bending and torsion should be well-balanced in order to produce a reasonable relation between numerical effort and overall accuracy. To provide greater flexibility, two different beam elements are developed. They differ only with regard to torsion. For the more sophisticated one, three instead of only two nodal displacements and interpolation functions are utilized to define the torsional displacement. This provides a more well-balanced accuracy (within the meaning of the statement made above). On the other hand, the more simple element may be advantageous when structural peculiarities require excessively refined subdividing into segments.

Nodal force quantities according to Fig. 1 and corresponding nodal displacements are used. For Element I, the force and displacement vectors are defined by:

$$\boldsymbol{\delta}^{I} = \begin{pmatrix} \delta_1 \\ \delta_2 \\ \delta_3 \\ \delta_4 \\ \hline \delta_5 \\ \delta_6 \end{pmatrix} = \begin{pmatrix} h_0 \\ h_l \\ h'_0 \\ h'_l \\ \hline \alpha_0 \\ \alpha_l \end{pmatrix}, \quad \mathbf{f}^{I} = \begin{pmatrix} f_1 \\ f_2 \\ f_3 \\ f_4 \\ \hline f_5 \\ f_6 \end{pmatrix}, \tag{1a}$$

and for Element II, by:

$$\boldsymbol{\delta}^{II} = \begin{pmatrix} \delta_1 \\ \delta_2 \\ \delta_3 \\ \delta_4 \\ \hline \delta_5 \\ \delta_6 \\ \delta_7 \end{pmatrix} = \begin{pmatrix} h_0 \\ h_l \\ h'_0 \\ h'_l \\ \hline \alpha_0 \\ \alpha_{l/2} \\ \alpha_l \end{pmatrix}, \quad \mathbf{f}^{II} = \begin{pmatrix} f_1 \\ f_2 \\ f_3 \\ f_4 \\ \hline f_5 \\ f_6 \\ f_7 \end{pmatrix}. \tag{1b}$$

The vertical displacement (bending) is interpolated by the well-known cubic Hermitian polynomials:[8]

$$\psi_1 = 1 - 3\xi^2 + 2\xi^3, \tag{2a}$$

$$\psi_2 = 3\xi^2 - 2\xi^3, \tag{2b}$$

$$\psi_3 = (\xi - 2\xi^2 + \xi^3)l, \tag{2c}$$

$$\psi_4 = (-\xi^2 + \xi^3)l, \tag{2d}$$

where:

$$\xi = \frac{x}{l}. \tag{3}$$

The torsional displacement of Element I is interpolated by the linear functions:

$$\psi_5^I = 1 - \xi, \tag{4a}$$

$$\psi_6^I = \xi. \tag{4b}$$

Finally, the torsional displacement of Element II is interpolated by:

$$\psi_5^{II} = 1 - 3\xi + 2\xi^2, \tag{5a}$$

$$\psi_6^{II} = 4\xi - 4\xi^2, \tag{5b}$$

$$\psi_7^{II} = -\xi + 2\xi^2. \tag{5c}$$

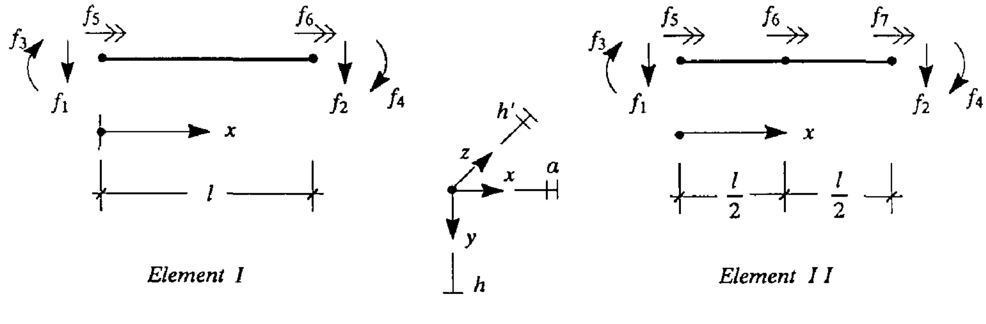

Fig. 1. Two finite beam elements.

Element matrices

The presentation will be confined to aerodynamic matrices. The structural property matrices (stiffness, mass) are either known, or can be easily calculated from known integral expressions. They are completely stated in Ref. [1].

Mechanical description of the self-induced aerodynamic forces proceeds analogously to the description of forces induced by stiffness and mass inertia. That is, the aerodynamic forces correspond to a vector of nodal forces which can be related to the nodal displacement vector by a linear matrix operation. For this, it is assumed that the flow in each cross-section remains unaffected by the flow in adjoining sections (strip theory). The aerodynamic nodal force vector may be written:

$$\mathbf{f}_L = -\omega^2 \mathbf{a}\boldsymbol{\delta}, \tag{6}$$

where ω = circular frequency. In conformity with Eq. (1a,b), the aerodynamic matrix $\mathbf{a}$ is divided into submatrices:

$$\mathbf{a} = \begin{pmatrix} \mathbf{a}^{hh} & \mathbf{a}^{h\alpha} \\ \mathbf{a}^{\alpha h} & \mathbf{a}^{\alpha\alpha} \end{pmatrix}. \tag{7}$$

Taking recourse to the principle of virtual displacements, it is found that the coefficients of $\mathbf{a}$ are given by:

$$a_{ij}^{hh} = \pi \int_0^l \rho b^2 c_{hh} \psi_i \psi_j \,\mathrm{d}x, \tag{8a}$$

$$a_{ij}^{h\alpha} = \pi \int_0^l \rho b^3 c_{h\alpha} \psi_i \psi_j \,\mathrm{d}x, \tag{8b}$$

$$a_{ij}^{\alpha h} = \pi \int_0^l \rho b^3 c_{\alpha h} \psi_i \psi_j \,\mathrm{d}x, \tag{8c}$$

$$a_{ij}^{\alpha\alpha} = \pi \int_0^l \rho b^4 c_{\alpha\alpha} \psi_i \psi_j \,\mathrm{d}x, \tag{8d}$$

in which ρ = density of fluid; and b = half chord of the cross-section's aerodynamic contour [1]. The four complex aerodynamic coefficients $c_{mn} = c'_{mn} + ic''_{mn}$ (or the eight real coefficients c'_{mn}, c''_{mn}) must be determined theoretically or experimentally as functions of the reduced frequency:

$$k = \frac{\omega b}{v}; \quad w, k \in \boldsymbol{R}, \tag{9}$$

where v = wind speed.[9,10] These coefficients represent the influence of the aerodynamic contour. Their relation with the real coefficients introduced by Scanlan[11] is described by:

$$c'_{hh} \triangleq \cdot/\cdot\,, \quad c''_{hh} \triangleq \frac{4}{\pi} H_1^*, \tag{10a}$$

$$c'_{h\alpha} \triangleq \frac{8}{\pi} H_3^*, \quad c''_{h\alpha} \triangleq \frac{8}{\pi} H_2^*, \tag{10b}$$

$$c'_{\alpha h} \triangleq \cdot/\cdot\,, \quad c''_{\alpha h} \triangleq \frac{8}{\pi} A_1^*, \tag{10c}$$

$$c'_{\alpha\alpha} \triangleq \frac{16}{\pi} A_3^*, \quad c''_{\alpha\alpha} \triangleq \frac{16}{\pi} A_2^*. \tag{10d}$$

There are no equivalents in the notation of Ref. [11] for the real parts of c_{hh} and $c_{\alpha h}$. As indicated in Eq. (9), the investigation will usually be limited to the border case of purely sinusoidal flutter (simple harmonic motion).

Wind velocity, aerodynamic contour and thus also k, and the coefficients c_{mn} are supposed to be invariable along the element axis. Evaluation of the integrals leads to:

$$\mathbf{a}^{hh} = \pi \rho b^2 c_{hh} \frac{l}{420} \begin{pmatrix} 156 & 54 & 22l & -13l \\ 54 & 156 & 13l & -22l \\ 22l & 13l & 4l^2 & -3l^2 \\ -13l & -22l & -3l^2 & 4l^2 \end{pmatrix}, \tag{11}$$

which is valid for both Elements. Furthermore, the following expressions are obtained. For Element I:

$$\mathbf{a}_I^{h\alpha} = \pi \rho b^3 c_{h\alpha} \frac{l}{60} \begin{pmatrix} 21 & 9 \\ 9 & 21 \\ 3l & 2l \\ -2l & -3l \end{pmatrix}, \tag{12a}$$

$$\mathbf{a}_I^{\alpha h} = \pi \rho b^3 c_{\alpha h} \frac{l}{60} \begin{pmatrix} 21 & 9 & 3l & -2l \\ 9 & 21 & 2l & -3l \end{pmatrix}, \tag{12b}$$

$$\mathbf{a}_I^{\alpha\alpha} = \pi \rho b^4 c_{\alpha\alpha} \frac{l}{6} \begin{pmatrix} 2 & 1 \\ 1 & 2 \end{pmatrix}, \tag{12c}$$

and for Element II:

$$\mathbf{a}_{II}^{h\alpha} = \pi \rho b^3 c_{h\alpha} \frac{l}{60} \begin{pmatrix} 11 & 20 & -1 \\ -1 & 20 & 11 \\ l & 4l & 0 \\ 0 & -4l & -l \end{pmatrix}, \tag{13a}$$

$$\mathbf{a}_{II}^{\alpha h} = \pi \rho b^3 c_{\alpha h} \frac{l}{60} \begin{pmatrix} 11 & -1 & l & 0 \\ 20 & 20 & 4l & -4l \\ -1 & 11 & 0 & -l \end{pmatrix}, \tag{13b}$$

$$\mathbf{a}_{II}^{\alpha\alpha} = \pi \rho b^4 c_{\alpha\alpha} \frac{l}{30} \begin{pmatrix} 4 & 2 & -1 \\ 2 & 16 & 2 \\ -1 & 2 & 4 \end{pmatrix}. \tag{13c}$$

These submatrices are joined to the complete aerodynamic matrices in accordance to Eq. (7). Apart from scalar factors, the diagonal blocks $\mathbf{a}^{hh}$ and $\mathbf{a}^{\alpha\alpha}$ agree with the corresponding diagonal blocks of mass matrices for elements with uniformly distributed mass.

The paper by Bruno *et al.* [12] gives an aerodynamic matrix for an element which corresponds to Element I as described in this paper. Scanlan's notation is used, in which c'_{hh} and $c'_{\alpha h}$ are neglected. Except for this, the aerodynamic matrix given in Ref. [12] can be exactly transformed into expressions (11) and (12).

Equations of motion and solution

When transforming and adding the nodal forces into global force vectors, the dynamic equilibrium condition may be expressed as:

$$\mathbf{F}_S + \mathbf{F}_D + \mathbf{F}_I + \mathbf{F}_L = 0. \tag{14}$$

The global force vectors $\mathbf{F}_S$, $\mathbf{F}_I$, $\mathbf{F}_L$ can be related to the global displacement vector $\boldsymbol{\Delta}$ by the following linear matrix operations:

$$\mathbf{F}_S = \mathbf{K}\boldsymbol{\Delta}, \tag{15a}$$

$$\mathbf{F}_I = \mathbf{M}\ddot{\boldsymbol{\Delta}}, \tag{15b}$$

$$\mathbf{F}_L = -\omega^2\mathbf{A}(k)\boldsymbol{\Delta}. \tag{15c}$$

The global stiffness matrix, mass matrix and aerodynamic matrix defined by these equations result from the respective element matrices in the usual way.

It is assumed here that the global vector of structural damping may be written:

$$\mathbf{F}_D = \mathbf{C}\boldsymbol{\Delta}, \tag{16}$$

where $\mathbf{C}$ = global damping matrix. In the case of weak damping (say $g \leq 0.05$), the approximative relation:

$$\mathbf{C} = ig\mathbf{K}, \tag{17}$$

can be used, in which g = overall damping coefficient. Thus, the internal damping forces are introduced as being of a magnitude proportional to the restoring forces induced by elasticity and in phase with the velocity.[6]

When substituting the global force vectors in Eq. (14) and using the exponential solution function:

$$\boldsymbol{\Delta}(t) = \bar{\boldsymbol{\Delta}}e^{i\omega t}, \tag{18}$$

the matrix-eigenvalue problem:

$$[(1+ig)\,\mathbf{K} - \omega^2(\mathbf{M} + \mathbf{A}(k))]\,\boldsymbol{\Delta} = 0, \tag{19}$$

is obtained which is linear in relation to ω^2. In addition to ω, this equation also depends on the reduced frequency k. When k is fixed, solving Eq. (19) yields n eigenvalues ω_j^2 which generally are complex. In the border case of sinusoidal flutter, the corresponding ω_j^2 is real and positive. Hence, k must be fixed repeatedly until this condition is met. The critical wind speed then follows from Eq. (9). For the purpose of practical flutter prediction, the lowest possible wind speed resulting in this way has to be determined.

If wind speed or cross-section is not uniform along the bridge span, the procedure can easily be generalized. The structure is divided into a sufficient number of elements with each having uniform, but possibly different aerodynamic (and structural) properties. Each element p has its own reduced frequency k_p. The mutual relationship of all k_p, however, is defined by the spatial distribution of wind speed and deck width. Hence, they can be expressed as functions of only one arbitrary reference value k^*. In the procedure described above, k^* then replaces k.

EXAMPLE CALCULATIONS

Based on the given theory, a computer program for spatial flutter calculation has been developed. Consider the uniform beam shown in isometric view in Fig. 2, which is subjected to a stream perpendicular to the beam axis. The supports constrain it against vertical and torsional displacements at its ends.

Results of a flutter calculation by means of finite elements are compared to (theoretically) exact results. The following system parameters are assumed:

$$\mu = \frac{m}{\pi\rho b^2} = 50, \tag{20a}$$

$$r = \frac{1}{b}\sqrt{\frac{I}{m}} = 0.75, \tag{20b}$$

where μ = relative density; r = reduced mass radius of gyration; m = mass per unit length; and I = mass moment of inertia per unit length. For the ratio of the lowest torsional natural frequency to the lowest vertical-bending natural frequency, the two different values:

$$\varepsilon_{11} = \frac{\omega_{\alpha 1}}{\omega_{h1}} = \begin{cases} 1.3 \rightarrow \text{System A} \\ 2.0 \rightarrow \text{System B}, \end{cases} \tag{20c}$$

are used. The damping coefficient is:

$$g = \begin{cases} 0 \rightarrow \text{undamped} \\ \dfrac{0.20}{\pi} \rightarrow \text{damped.} \end{cases} \tag{20d}$$

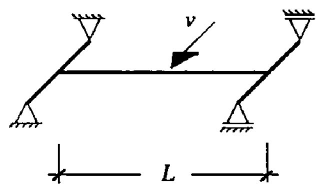

Fig. 2. System configuration.

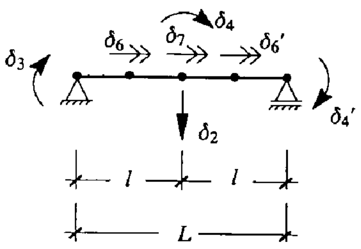

Fig. 3. Modeling with two elements type II.

By utilizing the theoretical aerodynamic coefficients given by Theodorsen[9] (valid for a thin aerofoil), the dimensionless aeroelastic quantities:

$$k = \frac{\omega b}{v}, \tag{21a}$$

$$\bar{\omega} = \frac{\omega}{\omega_{h1}}, \tag{21b}$$

$$\zeta = \frac{v}{\omega_{h1} b}, \tag{21c}$$

are evaluated for the border case of sinusoidal flutter. In order to facilitate numerics, Theodorsen's circulation function $C(k)$ is approximated by expressions given in Ref. [12].

Firstly, evaluation of aeroelastic quantities is based upon generalized 2-DOF systems. Because the modes of torsional and vertical vibration in vacuum of the investigated spatial system are identical, exact results are obtained.[1] Secondly, the beam is modeled by two finite elements type II (Fig. 3). Results of this analysis are presented in Table 1; deviations relative to exact results are given in brackets. Evidently, even with only a small number of elements, good accuracy is achieved.

Further investigation was dedicated to the flutter behavior of a long-span cable-stayed bridge (Fig. 4) whose modes of torsional and vertical vibration in vacuum differ.[1] Torsional rigidity and, consequently, the ratios $\varepsilon_{ij} = \omega_{\alpha i}/\omega_{hj}$ of natural frequencies for torsional and vertical-bending modes in vacuum were varied. Based on FE-models, as well as on generalized 2-DOF systems, critical wind speeds were evaluated using the theoretical aerodynamic coefficients.

The stability chart (Fig. 5) summarizes results of these comparative analyses. Calculated critical wind speeds are plotted versus frequency ratio ε_{11}. Simplified calculation by means of 2-DOF systems always yields the lowest critical wind speed. For a small parameter range near $\varepsilon_{11} = 1.1$, FE-modeling of the spatial system provided a theoretical speed increase of up to 150%. Significant increases over larger parameter ranges result from mode and frequency combinations (as input quantities for simplified 2-DOF calculation) that in spatial FE-analysis turn out to be irrelevant.

POTENTIAL APPLICATIONS

Aside from non-affinity of vacuum mode shapes, there may exist other system or environmental properties that make a spatial flutter analysis highly desirable.

For cable-supported bridges, torsional and transverse free-vibration response can be strongly coupled. The corresponding natural frequencies might be considerably lower than the natural frequencies of purely torsional motion (of comparable systems without torsional–transverse coupling). Simplified 2-DOF calculation based upon such natural frequencies will yield rather conservative results as long as inertia and damping contributions of the transverse motion component are not properly taken into account. One way of considering these contributions is a spatial flutter analysis utilizing finite beam elements. Including freedom of transverse motion in the here-described beam elements is straightforward as long as influence of transverse motion on aerodynamic forces is neglected.

Furthermore, need for spatial flutter analysis can result from strong variation of structural or aerodynamic properties along the bridge span. At some bridge sites, occurring wind velocity is strongly non-uniformly distributed. In future bridge design, variation of the cross-section's aerodynamic con-

Table 1. Results of aeroelastic finite-element calculation

		Undamped		Damped	
System A	k	0.303 955 8	(+0.01%)	0.218 212 4	(−0.03%)
	$\bar{\omega}$	1.165 036	(+0.38%)	1.107 838	(+0.38%)
	ζ	3.832 913	(+0.37%)	5.076 879	(+0.41%)
System B	k	0.189 785 6	(−0.01%)	0.158 485 8	(−0.01%)
	$\bar{\omega}$	1.517 740	(+0.37%)	1.404 679	(+0.37%)
	ζ	7.997 129	(+0.38%)	8.863 124	(+0.38%)

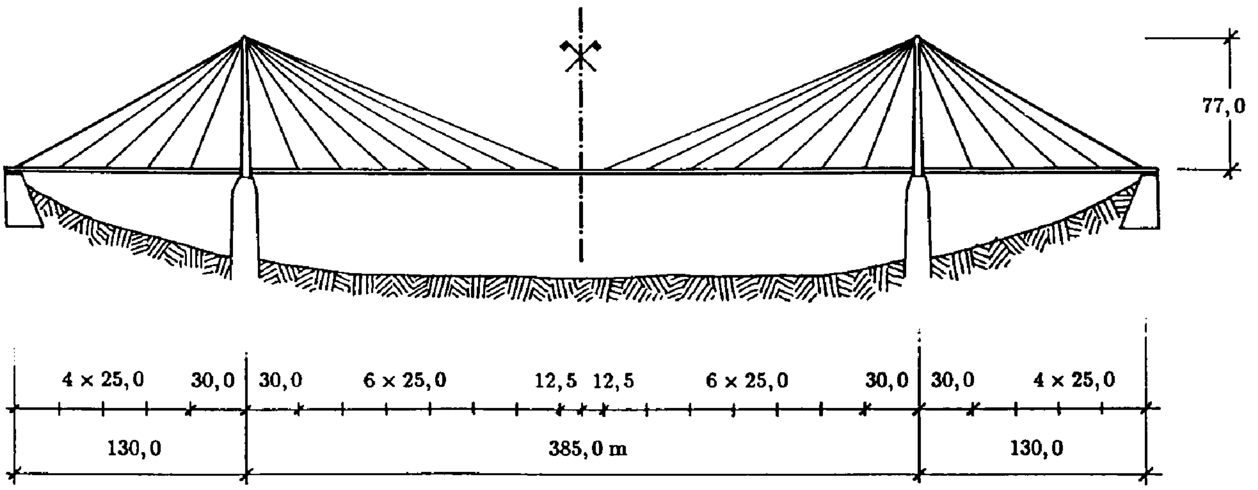

Fig. 4. Cable-stayed bridge configuration.

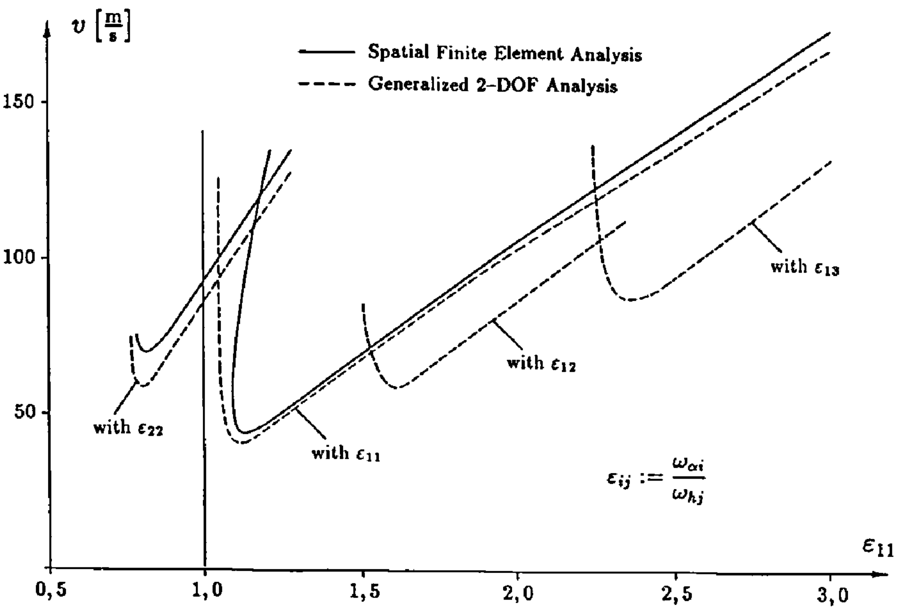

Fig. 5. Critical wind speed vs frequency ratio.

tour may be considered. Both of these peculiarities can be handled by using the here-given finite beam elements and the outlined algorithm.

CONCLUSIONS

Two finite beam elements were presented that are suitable for flutter calculation of line-like three-dimensional structures such as bridges. Formulation and solution of the resulting MDOF equations of motion were described. By comparing results obtained with finite elements to exact results, the efficiency and accuracy of the described method were demonstrated. Its application to bridge flutter prediction leads to critical wind speeds which considerably exceed the speeds obtained from simplified calculation by means of generalized 2-DOF systems.

Acknowledgements—This paper is based on the author's research at the Institute for Structural Design, University of Stuttgart. Support received from Professor Jörg Schlaich, Mr Knut Gabriel, and the Institute staff is gratefully acknowledged.

REFERENCES

1. U. Starossek, *Brückendynamik—Winderregte Schwingungen von Seilbrücken (Bridge Dynamics—Wind-induced Vibration of Cable-supported Bridges)*, Doctoral Thesis, Universität Stuttgart, 1991, Friedr. Vieweg und Sohn, Braunschweig, 1992.
2. U. Starossek, "Ein Beitrag zum Brückenflattern—Nachweis am ebenen Ersatzsystem und Einfluß des Profils (Contribution to the bridge flutter problem: prediction by means of generalized 2-DOF systems and influence of cross-sectional shape)," *Bauingenieur* **68**, 95–98 (1993).
3. F. Thiele, "Zugeschärfte Berechnungsweise der aerodynamischen Stabilität weitgespannter Brücken

(Sicherheit gegen winderregte Flatterschwingungen)," *Der Stahlbau* **45**, 359–365 (1976).
4. R. L. Bisplinghoff and H. Ashley, *Principles of Aeroelasticity*, John Wiley, New York, 1962.
5. H. W. Försching, *Grundlagen der Aeroelastik*, Springer, Berlin, 1974.
6. Fr. Bleich, "Dynamic instability of truss-stiffened suspension bridges under wind action," *Transactions, ASCE* **114**, 1177–1232 (1949).
7. J. R. Richardson, "Advances in techniques for determining the aeroelastic characteristics of suspension bridges," *Proceedings of the Fourth International Conference on Wind Effects on Buildings and Structures, Heathrow* 1975, Session 3, 251–258, 1975.
8. R. W. Clough and J. Penzien, *Dynamics of Structures*, McGraw-Hill, New York, 1975.
9. Th. Theodorsen, "General theory of aerodynamic instability and the mechanism of flutter," *National Advisory Committee for Aeronautics, Washington, D.C.*, Technical Report No. 496, 413–433, 1934.
10. N. Ukeguchi, H. Sakata and H. Nishitani, "An investigation of aeroelastic instability of suspension bridges," *Symposium on Suspension Bridges, Lisbon* 1966, Paper No. 11, 1966.
11. R. H. Scanlan, "An examination of aerodynamic response theories and model testing relative to suspension bridges," *Proceedings of the Third International Conference on Wind Effects on Buildings and Structures, Tokyo* 1971, Part IV, 941–951, 1971.
12. D. Bruno, A. Leonardi and F. Maceri, "On the nonlinear dynamics of cable-stayed bridges," *Proceedings of the International Conference on Cable-stayed Bridges, Bangkok*, 18–20 November 1987, **1**, 529–544, 1987.
13. J. Argyris and H.-P. Mlejnek, *Die Methode der Finiten Elemente. Band III: Einführung in die Dynamik*, Friedr. Vieweg and Sohn, Braunschweig, 1988.
14. K. Klöppel and F. Thiele, "Modellversuche im Windkanal zur Bemessung von Brücken gegen die Gefahr winderregter Schwingungen," *Der Stahlbau* **36**, 353–365 (1967).